



**HAL**  
open science

## Detection of biofilm formation by ultrasonic Coda Wave Interferometry

Bowei Chen, Marwan Abdallah, Pierre Campistron, Emmanuel Moulin, Dorothee Debavelaere-Callens, Simon Khelissa, Pascal Debreyne, Nour-Eddine Chihib, Guillaume Delaplace

### ► To cite this version:

Bowei Chen, Marwan Abdallah, Pierre Campistron, Emmanuel Moulin, Dorothee Debavelaere-Callens, et al.. Detection of biofilm formation by ultrasonic Coda Wave Interferometry. *Journal of Food Engineering*, 2021, *Journal of Food Engineering*, 290, pp.110219. 10.1016/j.jfoodeng.2020.110219 . hal-03049067

HAL Id: hal-03049067

<https://hal.univ-lille.fr/hal-03049067>

Submitted on 22 Aug 2022

**HAL** is a multi-disciplinary open access archive for the deposit and dissemination of scientific research documents, whether they are published or not. The documents may come from teaching and research institutions in France or abroad, or from public or private research centers.

L'archive ouverte pluridisciplinaire **HAL**, est destinée au dépôt et à la diffusion de documents scientifiques de niveau recherche, publiés ou non, émanant des établissements d'enseignement et de recherche français ou étrangers, des laboratoires publics ou privés.



Distributed under a Creative Commons Attribution - NonCommercial 4.0 International License

# 1 Detection of biofilm formation by ultrasonic Coda Wave 2 Interferometry

3 Bowei Chen<sup>a</sup>, Marwan Abdallah<sup>b</sup>, Pierre Campistron<sup>a</sup>, Emmanuel Moulin<sup>a,\*</sup>,  
4 Dorothée Callens<sup>a</sup>, Simon Oussama Khelissa<sup>b</sup>, Pascal Debreyne<sup>b</sup>, Nour-Eddine Chihib<sup>b</sup>  
5 and Guillaume Delaplace<sup>b</sup>

6 <sup>a</sup>Univ. Polytechnique Hauts-de-France, CNRS, Univ. Lille, ISEN, Centrale Lille, UMR 8520 - IEMN - Institut  
7 d'Électronique de Microélectronique et de Nanotechnologie, DOAE - Département d'Opto-Acousto-Électronique, F-59313  
8 Valenciennes, France

9 <sup>b</sup>INRA UR638, Processus aux Interfaces et Hygiène des Matériaux, BP 20039, F-59651 Villeneuve d'Ascq, France

10

## 11 ARTICLE INFO

13

### 14 Keywords:

15 Biofilm monitoring

16 Fouling detection

17 Coda Wave Interferometry

18 Ultrasonics

19

20

21

22

23

24

25

26

27

28

29

30

31

32

33

34

35

36

37

38

39

40

41

42

43

44

45

46

47

48

49

50

51

52

53

54

55

56

## ABSTRACT

The biofilm formation on food-contact-surfaces is a serious threat for public health and often results in huge human and economic losses. Thus, it is of importance to develop new strategies that allow the monitoring of the biofilm formation on food-contact-surfaces. Such strategies permit effective and timely countermeasures and, therefore, to avoid the microbiological risk and associated environmental impact due to cleaning processes. Therefore, this work investigated a non-invasive method for monitoring and detection of the biofilm formation using Coda Wave Interferometry (CWI) method. The principle of this method and the calculation of decorrelation coefficient based on the ultrasonic measurements were explained. The results underlined that our developed method is able to detect the early stage of the biofilm formation of *Staphylococcus aureus* on the stainless steel. Namely, it is shown that the bacterial cell kinetic is well captured by the evolution of the decorrelation coefficient as a function of incubation times. Overall, this work showed that this cost effective CWI method is a promising tool for the detection of early stage biofilm formation on food-contact-surfaces.

29

## 1. Introduction

The biofilms represent a great issue and have substantial implications in several process industries, such as food, drinking water, paper production, petroleum, nuclear power and marine industries Freeman, Lock, Marxsen and Jones (1990); Van Houdt and Michiels (2010); FRANK and Koffi (1990); Lens, O'Flaherty, Moran, Stoodley and Mahony (2003). In food sectors, the biofilm formation on food-contact surfaces is a major problem in terms of public health threats and economic losses Abdallah, Benoiel, Drider, Dhulster and Chihib (2014a). Such biofilms act as reservoirs of microorganisms which often lead to the dissemination of pathogens and, therefore, to foodborne infections. This fact was highlighted in several studies underlining that foodborne diseases are caused to a large extent by the biofilms formed on equipment surfaces Abdallah et al. (2014a). For example, it has been reported that more than 65% of all microbial infections in food area

\*Corresponding author

 [emmanuel.moulin@uphf.fr](mailto:emmanuel.moulin@uphf.fr) (E. Moulin)

ORCID(s):

40 are caused by biofilms. According to the [French institute of public health surveillance](#) (InVS) report of 2016  
41 InVs (2016), 1455 collective food poisoning have been reported in France, affecting 13997 persons, resulting  
42 in 634 hospitalizations and 3 deaths. In Europe, the report of the Global Burden of Foodborne Diseases  
43 underlined that more than 23 million Europeans become ill each year after consuming contaminated food  
44 leading to up to 5000 deaths Abdallah, Khelissa, Ibrahim, Benoliel, Heliot, Dhulster and Chihib (2015).  
45 Every year, up to 600 million people, or nearly 1 in 10 people in the world, become sick from eating  
46 contaminated food. These infections cause more than 420000 deaths. In addition to human losses, food-  
47 borne and health-related infections cause significant morbidity and economic losses. For example, it has  
48 been reported that the annual cost of nosocomial and foodborne infections in the United States is around  
49 \$ 16.6 and \$ 77.7 billion, respectively Abdallah et al. (2015).

50 In this regard, excessive cleaning and sanitization processes are constantly used in food industries in  
51 order to combat biofilms and to consistently meet hygienic manufacturing requirements Mussalli, Hecker,  
52 Padmarabhan, Kasper and Chow (1985). Such cleaning process often results in frequent process interruptions  
53 and related economic and environmental impacts. The environmental impact of cleaning and disinfection  
54 processes is mainly linked to the significant use of natural resources (ie water and energy), the use of chemicals  
55 (chloride, detergents, disinfectants) and the generation of CO<sub>2</sub> emissions and waste water Van Asselt, Vissers,  
56 Smit and De Jong (2005); MARTY (2001). Furthermore, such traditional sanitizing processes [often fail in the](#)  
57 [eradication](#) of biofilm and require additional enzymatic treatment in order to remove mature biofilms from  
58 food contact surfaces. In fact, the mature biofilms are known to be highly resistant to disinfecting/sanitizing  
59 agents and this is due to the interference of the self-produced exopolymeric matrix that hinders the diffusion  
60 of antimicrobials inside the biofilm. Thus, the biofilm early stage detection is of a vital importance to  
61 increase the likelihood of the biofilm eradication and to prevent the economic and environmental costs of  
62 cleaning processes. An efficient biofilm online detection/monitoring would allow the detection of the early  
63 stage of biofilm formation and to enable timely initiation of cleaning processes.

64 Along with issues caused by the biofilm formation or fouling on food-contact-surfaces, several works  
65 focused on the development of novel detection methods. These methods are usually based on agar plating  
66 or on metagenomic and metatranscriptomic studies Abdallah et al. (2014a). However, such methods are  
67 not effective at industrial level, [which is](#) due to the presence of viable but non-culturable (VBNC) cells in  
68 some biofilms and to the high cost of reagents and equipment. In addition, such methods do not provide  
69 online monitoring and may take hours or days in order to detect the biofilm formation of food-contact-  
70 surfaces. More recently, new methods, based on thermal pulse analysis, have been [developed in attempt](#)  
71 to detect the biofilm formation Fratamico, Annous and Guenther (2009). The principle of such methods is

72 based on implementation of sensors **that** measure the local thermal conductivity and heat variations due to  
73 the biofilm formation. However, these methods are somewhat limited because they are only able to detect  
74 thick deposits higher than few micrometers and, thus, cannot detect the early stage of biofilm formation  
75 Galiè, García-Gutiérrez, Miguélez, Villar and Lombó (2018). Other alternative technologies, such as the  
76 commercial quartz crystal microbalance (QCM) device analyzes, have been proposed Sprung, Wählich,  
77 Hüttl, Seidel, Meyer and Wolf (2009); Olsson, Mitzel and Tufenkji (2015). The adhesion of biofilms or  
78 other deposits to a quartz crystal changes the vibration frequency of such a surface. However, these sensors  
79 suffer from many complications regarding the temperature, the flow velocity and the nutrient presence in  
80 the bulk, which affect the frequency values. In addition, these sensors are disadvantageous in terms of  
81 their high cost (tens of thousands of dollars), limiting their use to lab-based studies. In addition, such  
82 detection techniques are usually invasive and based on the introduction of an external perturbation in the  
83 system, which are often not suitable for **the** hygienic requirements in food industries Withers (1996). Finally,  
84 even though other techniques such as electrochemical impedance spectroscopy Dheilly, Linossier, Darchen,  
85 Hadjiev, Corbel and Alonso (2008) or electric resistance measurement Chen, Li, Lin and Ozkan (2004) have  
86 demonstrated their efficiency for biofilm and **fouling monitoring**, the measurements necessitate a particular  
87 setup and cannot be easily implemented online.

88 Acoustic detection techniques have been widely used to detect defects Tandon and Choudhury (1999);  
89 Donskoy, Sutin and Ekimov (2001). In the field of fouling detection on food-contact-surfaces, some classic  
90 acoustic monitoring techniques have been proposed using different kinds of direct acoustic ultrasonic waves  
91 (longitude wave, transverse wave, surface wave,...) Lohr and Rose (2003); Merheb, Nassar, Nongailard,  
92 Delaplace and Leuliet (2007); da Silva, Wanzeller, Farias and Neto (2008); Withers (1994); Collier (2014).  
93 These techniques are mainly based on the measurement of reflection coefficient of transverse waves, the time  
94 of flight and attenuation of echoes. In the classic acoustic detection techniques, the sensitivity is generally  
95 limited by the wavelength of the direct acoustic wave. For thin layer detection, high frequency waves are  
96 required to achieve acceptable results. However, the increase of the frequency leads to the increase of atten-  
97 uation of acoustic wave energy. The high attenuation reduces the signal-to-noise ratio (SNR) and leads to an  
98 inaccurate detection. In order to overcome such sensitivity limit without modifying the signal wavelength,  
99 the Coda Wave Interferometry (CWI), which is known to provide good performances, can be used. Coda  
100 waves have already been applied in seismic Snieder (2002); Zhou, Huang, Rutledge, Fehler, Daley and Majer  
101 (2010), volcano monitoring Matsumoto, Obara, Yoshimoto, Saito, Ito and Hasegawa (2001); Ratdomopurbo  
102 and Poupinet (1995), concrete detection Hilloulin, Zhang, Abraham, Loukili, Grondin, Durand and Tournat  
103 (2014); Planès and Larose (2013) and other domain BALAA, Le Duff, Plantier and El Guerjouma (2009),

104 but never used with the aim of fouling contamination detection. Furthermore, our previous work underlined  
105 that this technique is able to detect manually deposited wax on stainless steel Chen, Callens, Campistron,  
106 Moulin, Debreyne and Delaplace (2018). However, the application of such technique in the detection of  
107 biofouling materials, such as biofilms, has never been achieved.

108 In this paper, the non-destructive ultrasonic monitoring technique using coda waves is explored in order  
109 to monitor a biofilm formation on a stainless steel substrate. For this study, *Staphylococcus aureus*, a Gram-  
110 positive bacterium, is used for the biofilm formation. This bacterium is known to cause serious health issues  
111 in food sectors. The principle of this ultrasonic method and signal processing is described. In particular,  
112 the computation of the decorrelation coefficient, which is used as an indicator of the biofilm detection, is  
113 plotted as a function of incubation time. Then, the evolution of decorrelation coefficient is compared to the  
114 kinetic of the biofilm formation, which is followed by the bacterial cell enumeration using the conventional  
115 plate-counting technique.

## 116 2. Principle of ultrasound coda processing

117 In classical ultrasound techniques, echographic measurements use only direct ultrasound waves to detect  
118 and characterize changes in medium properties. These waves are the ones that propagate directly from  
119 the source to the sensor via a unique reflection at a given interface, and they consequently appear in the  
120 first part of the signal recording (basic illustration for our biofilm application is shown in Figure 1-left). In  
121 applications where these changes will only introduce very low property contrast, these direct echos will be  
122 very slightly affected, which will make the detection hazardous.

123 On the contrary, multiply-reflected and multiply-scattered wavepackets will cumulate the effects intro-  
124 duced by the medium changes over several wave paths (Figure 1-right). These so-called “coda waves” will  
125 naturally appear later signal plot. Briefly, the medium is crossed one time by direct waves and several times  
126 by coda waves. This will result in a much higher sensitivity of the coda waves to small property changes  
127 (such as caused here by the biofilm formation and evolution) than the direct wavepackets.

128 Since coda corresponds to a superposition of waves propagating along various paths, it is difficult to  
129 analyze it using classical acoustic parameters such as time-of-flight, reflection and transmission coefficients.  
130 Instead, useful information will be extracted by quantifying coda signal changes or dissimilarities between  
131 two states of the medium. To that end, the decorrelation coefficient is used as an indicator of the dissimilarity  
132 between two recorded coda signals  $s_1$  and  $s_2$ , respectively. It is computed in a given time-window  $[t_0, t_1]$

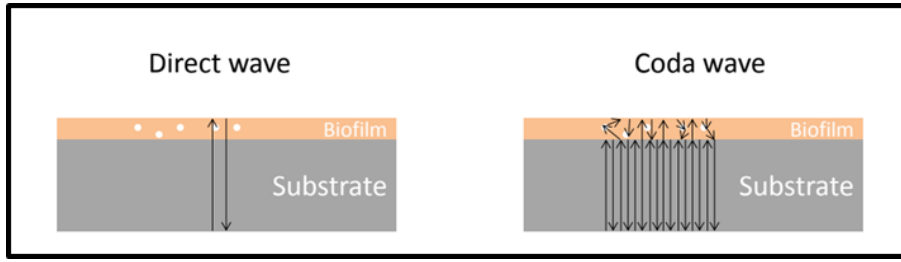


**Figure 1:** Schematic illustration of ultrasound wave propagation in the medium: direct waves (left) correspond to first reflected and backward propagated echoes, whereas coda waves (right) are multiply reflected and scattered inside the medium.

133 according to the following relation Zhang (2013):

$$D_{1,2} = 1 - \frac{\int_{t_0}^{t_1} s_1 s_2 dt}{\sqrt{\int_{t_0}^{t_1} s_1^2 dt \int_{t_0}^{t_1} s_2^2 dt}} \quad (1)$$

134 The second term in Eq. (1) corresponds to the normalized cross-correlation of  $s_1$  and  $s_2$  at zero lapse-time.  
 135 Mathematically, the value of  $D_{1,2}$  is between 0 and 2. Identical  $s_1$  and  $s_2$  signals lead to zero decorrelation  
 136 coefficient and nonzero values are an indicator of waveform shapes and phases differences between signals.  
 137 Hence, the value of  $D_{1,2}$  will be directly related to the degrees of state changes in the medium. Therefore,  
 138 in our application, its evolution during the monitoring procedure is expected to be linked to the biofilm  
 139 formation on the substrate. Typical behaviors of early (direct) wave signals and coda signals will be shown  
 140 in section 3.2, after presenting the experimental setup.

## 141 3. Materials and methods

### 142 3.1. Biofilm formation assay

143 The biofilm formation was performed on the upper side of circular stainless steel slides (3) Figure 2  
 144 (diameter : 4.1 cm; thickness: 1 mm). The CWI sensor is attached to the lower side of the stainless steel  
 145 slides in order to detect the biofilm formation (Figure 2). In order to obtain the formation of the biofilm, the  
 146 circular slide of stainless steel is placed in a static reactor (Figure 2-A and B). The reactor consists of several  
 147 assembled pieces of stainless steel and a rubber O-ring (Figure 2-(C)), as previously described by Abdallah  
 148 et al. Abdallah et al. (2015). The circular base of this reactor (5) is made of stainless steel and can receive  
 149 an O-ring (4) which is used to fit perfectly one circular test slide (3) (Figure 2-A). Then a stainless steel  
 150 cylinder (2) was placed in order to form the well of the biofilm formation. A collar clamp (6) was used to  
 151 provide tightness and a metal cover (1) was used to ensure the sterility of the closed system (Figure 2-C and

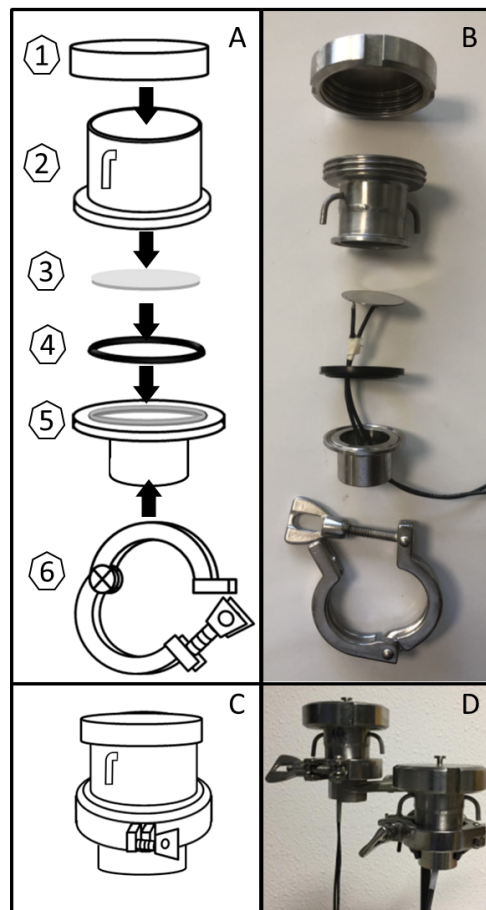


**Figure 2:** Description of the installation. A and B present schematics of the system assemblage; C and D present the assembled system: (1) metal cover; (2) stainless steel cylinder; (3) circular stainless steel slide; (4) rubber O-ring; (5) circular stainless steel base; (6) collar clamp.

152 D). Two similar reactors are used to evaluate the ability of the sensor for detecting the deposit formation  
 153 (Figure 2-D). The first one is for monitoring the biofilm formation (marked as reactor 1), and the second  
 154 one is used as a negative control or witness (marked as reactor 2).

155 Prior to their use, the reactors were cleaned and disinfected using ethanol 95% (v/v) to ensure sterility.  
 156 The formation of biofilm was performed as described by Abdallah et al Abdallah et al. (2015). The first step  
 157 of the biofilm formation was the bacterial adhesion to the surface. Then the formation of biofilm layers was  
 158 triggered by adding the culture medium in the wells and placing reactors in an incubator with a controlled  
 159 temperature. Biofilm formation was performed under the same conditions using separated reactors. Part of  
 160 reactors was used to perform bacterial counting using the reference method (plate counting) and the other  
 161 part was used to perform CWI monitoring. In details, step 1 was performed by the deposition of 5 mL of  
 162 bacterial suspension ( $10^7$  CFU/mL) in the well of reactor 1 and, then, incubated at 20°C for 1 h to allow  
 163 the bacterial adhesion to the substrate. For the negative control (or witness), 5 ml of sterile physiological



**Figure 3:** Photo of biofilm formed on the substrate of reactor 1

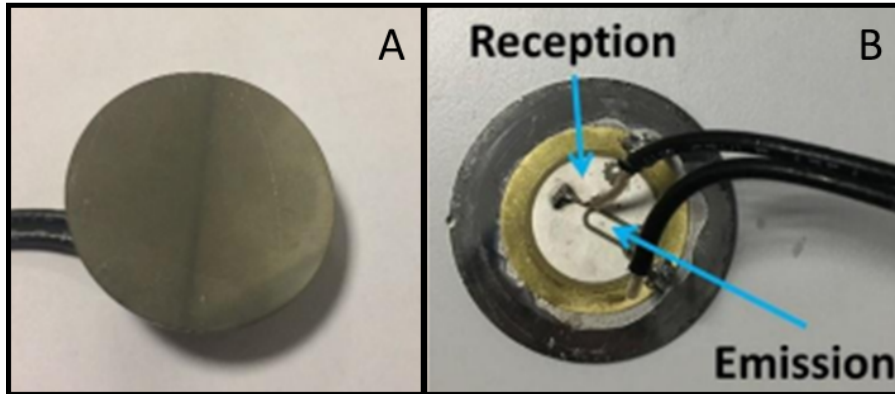
164 saline water were used. After 1h of bacterial adhesion, step 2 was started. For that, the 5 mL of bacterial  
 165 suspension were removed and the slides were washed twice using physiological saline water (8.5% of NaCl) in  
 166 order to remove loosely attached cells. These 5 ml were removed in order to reduce the number of floating  
 167 cells. Then 25 mL of Tryptone Soy Broth (TSB; Biokar Diagnostics, Pantin, France)) were deposited in each  
 168 well. Thereafter, reactors are sealed by lids and incubated at controlled temperature of 30°C to allow the  
 169 biofilm formation (Figure 3). The average thickness of biofilm layer, after 30 h, has been checked visually  
 170 and is around 50  $\mu\text{m}$  as measured by Abdallah et al. Abdallah et al. (2015). All experiments were done  
 171 under sterile environment to avoid undesired contamination and to control as much as possible the biofilm  
 172 growth.

173 The biofilm formation kinetics were investigated both with the plate count method and CWI monitoring,  
 174 for comparison. For the classic plate count method, which will serve as the reference method, stainless  
 175 steel slides were removed from the first part of reactors and placed in separated sterile containers Abdallah,  
 176 Chataigne, Ferreira-Theret, Benoliel, Drider, Dhulster and Chihib (2014b). The bacterial cells were detached  
 177 in 20 ml of phosphate buffer (100 mM) by vortexing for 30 s followed by a sonication at 37 kHz for 5 min.  
 178 Then tenfold serial dilutions of each bacterial suspension were made in tryptone salt broth (TS; Biokar  
 179 Diagnostics, Pantin, France). 100  $\mu\text{l}$  of each dilution were spread onto tryptic soy agar plates (TSA; Biokar  
 180 Diagnostics, Pantin, France). Agar plates were incubated at 37°C and the number of viable and culturable  
 181 cells was counted after 0, 6, 12, 18, 24 and 30 h of incubation. The results are expressed in log CFU/cm<sup>2</sup>  
 182 and represent the means of three independent experiments. The bacterial counts of bacterial cells after step  
 183 1 showed that the number of attached cells in reactor 1 was around 10<sup>5</sup> CFU/cm<sup>2</sup>. As expected, no adhered  
 184 bacterial cells were found in reactor 2 (witness or control condition).

**Table 1**

Biofilm biomasses as a function of incubation time

Time (h)	Biofilm biomass (Log $CFU/cm^2$ )
0	$5.1 \pm 0.2$
6	$5.7 \pm 0.1$
12	$6.2 \pm 0.2$
18	$7.0 \pm 0.1$
24	$7.9 \pm 0.4$
30	$8.1 \pm 0.3$

**Figure 4:** Piezoelectric transducer used for the acquisition. **A and B** present the upper and the lower faces, respectively.

### 185 3.2. Ultrasound acquisition

186 For the biofilm formation monitoring, biofilms were formed on stainless steel according to the protocol  
 187 described above. **A continuous ultrasound monitoring is applied in order to detect the different steps of**  
 188 **the biofilm formation in the reactors 1 and 2.** The signal acquisition system consists of 5 components: a  
 189 laptop PC with acquisition software (Matlab, instruments drivers), a waveform generator (Keysight 33600A  
 190 Series), an acquisition board (PicoScope 5000 Series), an amplifier with internal high-pass filters (**Eurosonics-**  
 191 **Mistras Group, 1 kHz-50 MHz frequency range, 40 dB gain**) and two transducers. The transducers used in  
 192 this experiment are low-cost piezoelectric patches (Figure 4), consisting of two separate electroded parts for  
 193 emission and reception. Their thickness resonance frequency is around 10 MHz. As mentioned above, they  
 194 are glued on the lower side of the circular stainless steel substrate as described in Figure 2. This device **was**  
 195 **used to monitor** the biofilm formation occurring on the upper side of the circular slides.

196 The excitation signal is one period of sinus at 10 MHz. The transducers convert the electrical signals to  
 197 ultrasound waves through piezoelectric effect. After propagation and multiple reflections and scattering in  
 198 the sample (see more detailed explanation below), parts of these waves are returned towards the transducer  
 199 and converted back into electrical signals at the reception electrode. After high-pass filtering above 1 kHz  
 200 (aimed at filtering out low frequency vibrations coming from the environment) and amplification, the received

201 signals are fed into the acquisition board with sampling frequency 125 MHz and recorded in the PC after  
 202 averaging over 100 signal acquisitions. This acquisition process is then repeated every five minutes, from the  
 203 beginning of biofilm formation and for a total monitoring duration of thirty hours. The biofilm formation on  
 204 the surface will modify the substrate/biofilm interface properties and therefore lead to subsequent changes of  
 205 reflected and back-scattered ultrasound signals. It is important to highlight here that even though bacterial  
 206 arrangement in the biofilm constitutes a disordered medium, which results in complex ultrasound coda  
 207 signals with intricated multi-path propagation, these signals are fully reproducible for a given biofilm state  
 208 (*i. e.* a given incubation time). Indeed, since the ultrasound sensor is fixed relatively to the medium, and  
 209 acquisition time of the signals is very small compared to the time scale of biofilm evolution, two signals  
 210 recorded at the same state of the medium are identical.

211 The changes related to the biofilm evolution are monitored using the coda processing explained in sec-  
 212 tion 2. To improve the signal-to-noise ratio, the signals are band-pass filtered with a certain frequency  
 213 band  $[f_1 f_2]$  around the excitation frequency  $f_0$ , prior to decorrelation estimation computed from Eq. (1).  
 214 For correct account of the frequency content, the width of time window  $\Delta t = t_1 - t_0$  should satisfy the  
 215 condition  $\Delta f \Delta t \gg 1$  (where  $\Delta f = f_2 - f_1$ ). In the following, as in other literature studies Payan, Garnier,  
 216 Moysan and Johnson (2009); Snieder (2004); Chen et al. (2018),  $\Delta t$  will be chosen to be at least 10 periods  
 217 of excitation signal. This will require the relative bandwidth to be larger than 10%.

218 To illustrate the effect of biofilm formation on the ultrasound signals, two recorded experimental signals  
 219 are plotted on Figure 5. The blue one is the reference signal, measured at initial state (before biofilm  
 220 formation). Time  $t = 0$  s corresponds to the instant of emission of the incident ultrasound signal and this  
 221 timebase reference is the same for all recordings. The red signal is recorded after 4 hours of biofilm formation.  
 222 It can be seen that the signal parts corresponding to direct waves (the first part in the signals with strong  
 223 amplitude) did not change with the variation of the surface state. However, in the coda part (next to the  
 224 direct waves around  $8 \mu\text{s}$  with weaker amplitude), there is a remarkable difference between the perturbed  
 225 signal and the reference signal. Obviously, coda waves are more suitable for detection of the state change of  
 226 medium than direct waves (Figure 5).

### 227 3.3. Environmental temperature

228 Acoustic waves are sensitive and influenced by temperature changes, in particular when using codas.  
 229 Therefore, a monitoring of temperature in the incubator is carried on using a thermometer at the same time  
 230 as the ultrasound acquisition. Since the signal recording time is very short and the biofilm formation is  
 231 very slow, the temperature change of sample and the growth of biofilm during one single acquisition can be

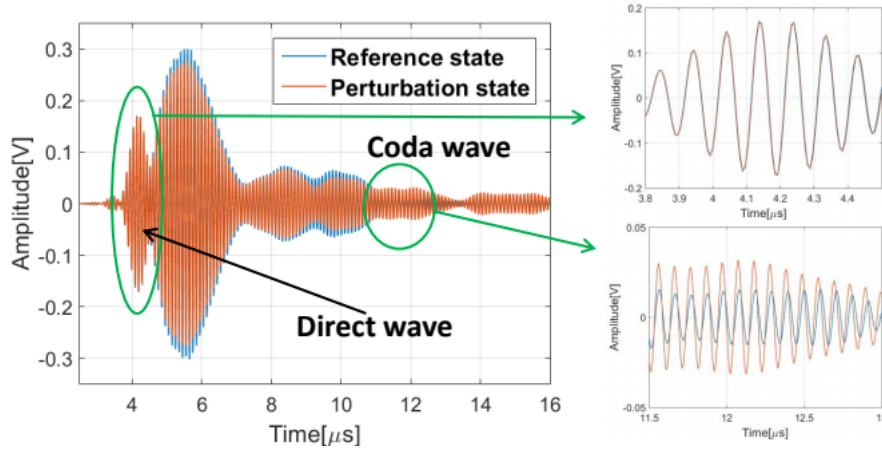


**Figure 5:** Two signals obtained in the experiment of monitoring the biofilm formation, representing two different sample states: Reference state (blue) and after 4 hours incubation (red)

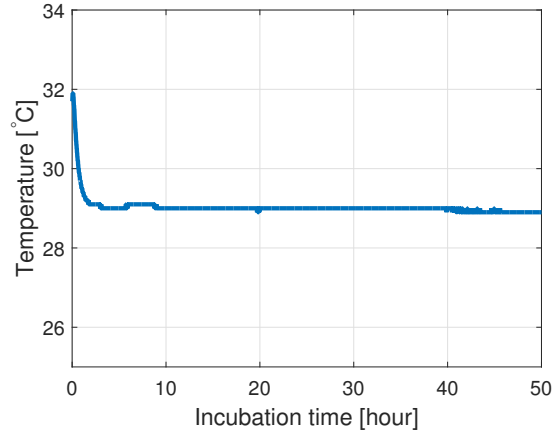


**Figure 6:** Evolution of the temperature in the incubator during the measurement.

232 neglected.

233 Temperature evolution measured during the biofilm formation in the reactor is shown in Figure 6-A. The  
 234 curve shows that temperature inside the reactor stabilizes approximately after two hours of the beginning  
 235 of incubation period. Therefore, the initial (or reference) state for the decorrelation coefficient estimation is  
 236 defined at two hours of incubation time, in order to avoid the influence of temperature changes.

## 237 4. Results and discussion

238 Two series of signals are obtained from reactors 1 and 2 and are recorded from 2 hours of incubation time  
 239 (taken as reference) with an interval time of 5 minutes. First, all these signals are numerically band-pass  
 240 filtered between 9 and 11 MHz (relative bandwidth 20%) and then decorrelation coefficients between the

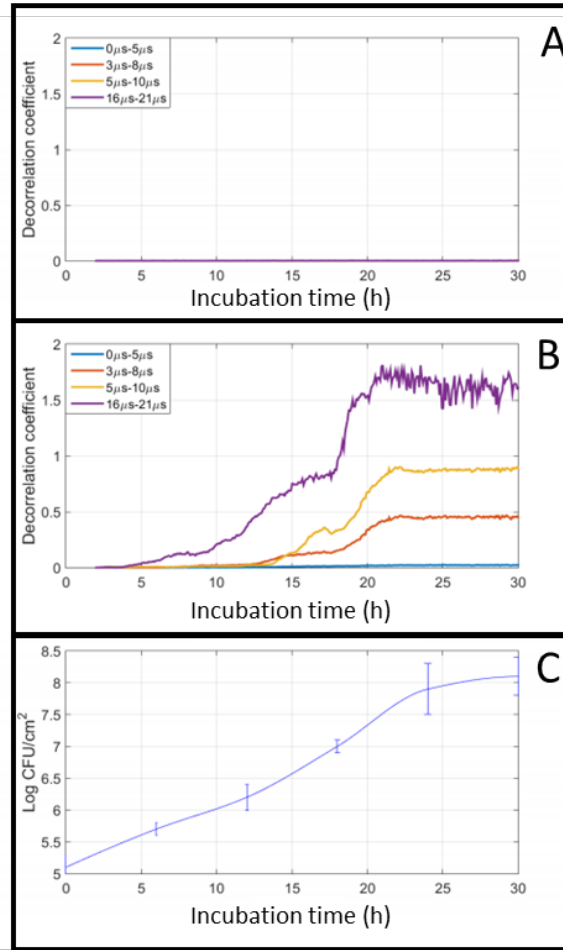


**Figure 7:** Decorrelation coefficient evolution as a function of incubation time for: A presents the control sample, B presents the biofilm formation sample, with different time windows:  $0 \mu s - 5 \mu s$ ,  $3 \mu s - 8 \mu s$ ,  $5 \mu s - 10 \mu s$ ,  $16 \mu s - 21 \mu s$  (frequency band 9 MHz-11 MHz); C presents the kinetic of *S. aureus* biofilm formation on stainless steel substrate.

241 reference signal and every subsequent **signal** is computed using Eq. (1) for sliding time-windows of duration  
 242  $\Delta t = 5 \mu s$ . This satisfies the conditions mentioned above on frequency bandwidth and time-window duration.

243 Figure 7-A and B show the evolution of the decorrelation coefficient as a function of incubation time for  
 244 the control and the biofilm **formation** samples, respectively. In both cases, decorrelation values **which are**  
 245 computed in four time-windows, are shown:  $0 \mu s - 5 \mu s$ ,  $3 \mu s - 8 \mu s$ ,  $5 \mu s - 10 \mu s$ ,  $16 \mu s - 21 \mu s$ .

246 **In the negative control reactor (Figure 7-A), the decorrelation coefficients are close to 0 for any incubation**  
 247 **time and selected time window.** This indicates the absence of any significant change from the initial surface  
 248 property state. This is coherent with the absence of biofilm formation, checked with naked eyes, on the  
 249 negative control substrate. In addition, these results confirm that no apparent variable factor, especially the  
 250 temperature, other than the biofilm formation on substrate influence the propagation of acoustic waves.

251 On the contrary, the results in Figure 7-B show that the decorrelation coefficients of biofilm monitoring

252 sample **increased significantly as the incubation time increased** . It also shows that the sensitivity of the state  
253 change detection depends on the time windows. The first window ( $0 \mu s - 5 \mu s$ ) is not sensitive at all since  
254 the decorrelation coefficients are close to 0. On the contrary and for the other time windows, corresponding  
255 to later parts of the coda, significant increases of the decorrelation coefficient can be observed. Finally,  
256 the decorrelation coefficients become stable after about 22 hours, which is probably due to the reaching of  
257 quasi-steady state of the biofilm formation.

258 In order to verify the correlation between the evolution curves in Fig. 7-B and the biofilm formation on  
259 substrate, the kinetic of *S. aureus* biofilm formation on the stainless steel was investigated by enumeration of  
260 biofilm cells on agar plates, as explained in Sec. 3.1. **The results are presented in Fig. 7-C, as mean values and**  
261 **the standard error to the mean (SEM). Data analysis was performed using Sigma Plot 11.0 (Systat Software,**  
262 **USA), using one-way ANOVA (Tukey's method) to determine the significance of differences.** These results  
263 showed that the counts of the initial adhered bacteria were in the range of  $5 \log \text{CFU}/\text{cm}^2$  (Table 1). They  
264 also showed that the biofilm biomasses increased with the increase of the incubation time and reached the  
265 steady state around 24 h of incubation time. In fact, the biofilm biomasses were stable and in the range of  
266  $8 \log \text{CFU}/\text{cm}^2$  (Figure 7-C). The biomass evolution could be compared with the decorrelation coefficient  
267 (Figure 7-B). Indeed, the data of the bacterial cell enumeration are well described by the decorrelation  
268 coefficient evolution.

269 Changes in the liquid nutrient medium during the bacterial growth could be another factor affecting the  
270 decorrelation coefficient. However, as soon as a biofilm is forming at the substrate-medium interface, the  
271 reflection coefficient will be essentially affected by the cell deposit on the substrate surface and its interfacial  
272 adhesion properties. Therefore, we are confident that the decorrelation coefficient is directly and essentially  
273 associated to the biofilm evolution, which the good matching between curves of Figure 7-B and Figure 7-C  
274 tends to confirm. These data proved that this method has the potential to detect and monitor **the early stage**  
275 **of the biofilm formation on a substrate in a non-invasive way, and apparently with an accuracy comparable**  
276 **with more classical and more invasive methods, though this point will have to be investigated in more details**  
277 **in future works.**

278 Finally, we will conclude this discussion by a short focus on temperature influence. As explained, the  
279 coda decorrelation results shown above correspond to constant temperature conditions (stabilization after  
280 two hours of incubation time). We present now in Figure 8-A the evolution of the decorrelation coefficient  
281 for the control sample during the first five hours of incubation time. For convenience temperature recorded  
282 at the same times is plotted again on Figure 8-B.

283 **As expected, the decorrelation coefficient varies when temperature changes, even in the absence of biofilm**

## Biofilm detection using CWI

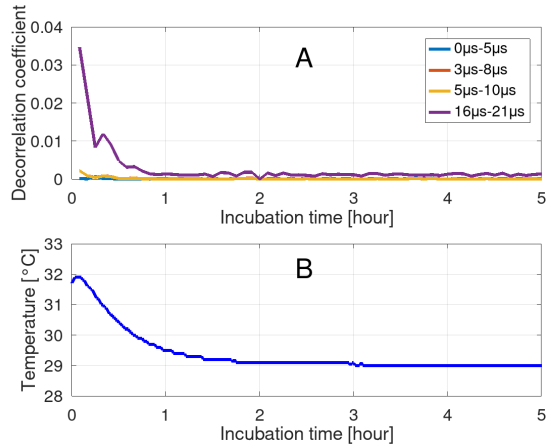


**Figure 8:** Influence of temperature on coda decorrelation. A: evolution of the decorrelation coefficient for the control sample. B: evolution of the temperature in the incubator during the measurement.

284 evolution. This validates the choice of waiting after two hours of incubation to avoid any temperature-  
285 induced decorrelation during biofilm monitoring. However we can also see that these variations are relatively  
286 moderate compared to those induced by the biofilm (Fig. 7-B). Quantitatively, for a temperature change  
287 of approximately 3 °C, the relative variation of the decorrelation coefficient is of the order of 2%, relatively  
288 to the full-scale of biofilm-induced variation. This means that even a variation of a few °C would only  
289 introduce a small error in the biofilm monitoring decorrelation curves. This is clearly encouraging for  
290 realistic application cases, though this point will obviously necessitate further studies.

## 291 5. Conclusion

292 The detection of biofilm formation on surfaces is of critical importance to sectors that directly affect  
293 human health. In fact, biofilm represents a reservoir of pathogens which results in serious human infections.  
294 Thus, an efficient biofilm monitoring on surfaces, commonly used in food and medical sectors, is needed in  
295 order to reduce the microbiological risks and associated human and economic losses. In this context, our  
296 work described a monitoring method which is based on Coda Wave Interferometry to detect the biofilm  
297 formation on stainless steel.

298 The principle of this monitoring technique is to compare the acoustic signals received at different in-  
299 stants. Decorrelation coefficient of multiply-reflected or scattered (coda) waves is used as an indicator of  
300 state changes in the samples. The method described herein presents several advantages over conventional  
301 methods based on optical, heat transfer, pressure drop, fluid dynamic gauging, direct weighing and thickness  
302 measurements. Indeed, conventional methods are usually invasive. On the contrary, the method described  
303 in this paper is non-invasive, cheap and easy to apply in food and medical environments. In addition, this

304 method is highly sensitive in the detection of the early stage of the biofilm growth. A bacterial biomass  
305 of  $5 \log \text{CFU}/\text{cm}^2$  appears to be enough to trigger a significant evolution of decorrelation coefficient (Fig-  
306 ure 7). Indeed, a 0.1 unit has been recorded and represents at least 5 % of signal variation of the value of  
307 decorrelation coefficient which theoretically varies between 0 and 2 units.

308 Our results show that this technique has the potential for performing continuous real-time biofilm detec-  
309 tion and monitoring in sealed opaque equipment. In addition, this method interestingly succeeded to detect  
310 the early stage of biofilm formation. In fact, the decorrelation coefficient started increasing from a bacterial  
311 concentration of  $10^5 \text{CFU}/\text{cm}^2$ .

312 This technique has some limitations which can be easily addressed. First, it allows only a local monitoring  
313 of biofilm formation (i.e. a small monitoring area of food contact surface). The use of multiple, judiciously  
314 distributed sensors could overcome this issue. Second, the technique is sensitive to temperature changes  
315 since this will affect the ultrasound coda properties. Though this is not a problem in applications where  
316 thermostatic control is ensured, this aspect could limit the extension of application range **in cases where**  
317 **significant temperature changes cannot be avoided**. A possible way to mitigate the impact of temperature  
318 changes **and to improve the accuracy of detection**, could be the use of multiple reference signals, recorded  
319 at different temperatures. Thus, by measuring the temperature simultaneously with the ultrasound codas,  
320 decorrelation coefficients related **recorded temperature** could be computed. This work is currently under  
321 progress. Finally, further studies will have to be conducted in order to quantify precisely the influence of  
322 the liquid medium properties.

## 323 Acknowledgements

324 The work on biofilm is carried out at the INRA (National Institute of Agronomic Research) in collabo-  
325 ration with the IEMN-DOAE (Institute of Electronics, Microelectronics and Nanotechnol-ogy - Department  
326 Opto-Acousto-Electronics). This research is funded by the Hauts-de-France Region (Grant number 15-CS-  
327 15-477) and the University Polytechnique Hauts-de-France (UPHF). **Furthermore, immediate continuation**  
328 **of this work and future applications to realistic case studies of biofilm-induced corrosion will be possible in**  
329 **the European Interreg 2 Seas project SOCORRO.**

## 330 References

- 331 Abdallah, M., Benoliel, C., Drider, D., Dhulster, P., Chihib, N.E., 2014a. Biofilm formation and persistence on abiotic surfaces  
332 in the context of food and medical environments. *Archives of Microbiology* 196, 453–472. doi:10.1007/s00203-014-0983-1.
- 333 Abdallah, M., Chataigne, G., Ferreira-Theret, P., Benoliel, C., Drider, D., Dhulster, P., Chihib, N.E., 2014b. Effect of  
334 growth temperature, surface type and incubation time on the resistance of staphylococcus aureus biofilms to disinfectants.

- 335 Applied Microbiology and Biotechnology 98, 2597–2607. URL: <https://doi.org/10.1007/s00253-013-5479-4>, doi:10.1007/  
336 s00253-013-5479-4.
- 337 Abdallah, M., Khelissa, O., Ibrahim, A., Benoliel, C., Heliot, L., Dhulster, P., Chihib, N.E., 2015. Impact of growth temper-  
338 ature and surface type on the resistance of *Pseudomonas aeruginosa* and *Staphylococcus aureus* biofilms to disinfectants.  
339 International Journal of Food Microbiology 214, 38–47. doi:10.1016/j.ijfoodmicro.2015.07.022.
- 340 BALAA, E., Le Duff, A., Plantier, G., El Guerjouma, R., 2009. Interférométrie par onde de coda: Effet de la température sur  
341 la propagation d'ondes acoustiques dans une plaque d'aluminium, in: XXIIe Colloque GRETSI (Traitement Du Signal et  
342 Des Images), Dijon (FRA), 8-11 Septembre 2009, GRETSI, Groupe d'Etudes du Traitement du Signal et des Images.
- 343 Chen, B., Callens, D., Campistron, P., Moulin, E., Debreyne, P., Delaplace, G., 2018. Monitoring cleaning cycles of fouled  
344 ducts using ultrasonic Coda Wave Interferometry (CWI). Ultrasonics 96, 263–260. doi:10.1016/j.ultras.2018.12.011.
- 345 Chen, X.D., Li, D.X., Lin, S.X., Ozkan, N., 2004. On-line fouling/cleaning detection by measuring electric resistance equipment  
346 development and application to milk fouling detection and chemical cleaning monitoring. Journal of Food Engineering 61,  
347 181–189. doi:10.1016/S0260-8774(03)00085-2.
- 348 Collier, N., 2014. Développement d'un Outil Ultrasonore de Caractérisation Des Propriétés d'adhésion de Milieux Modèles  
349 Avec Application Aux Dépôts Laitiers. Ph.D. thesis. Lille 1.
- 350 Dheilly, A., Linossier, I., Darchen, A., Hadjiev, D., Corbel, C., Alonso, V., 2008. Monitoring of microbial adhesion and biofilm  
351 growth using electrochemical impedancemetry. Appl. Microbiol. Biotechnol. 79, 157–164.
- 352 Donskoy, D., Sutin, A., Ekimov, A., 2001. Nonlinear acoustic interaction on contact interfaces and its use for nondestructive  
353 testing. NDT & E International 34, 231–238. doi:10.1016/S0963-8695(00)00063-3.
- 354 FRANK, J.F., Koffi, R.A., 1990. Surface-adherent growth of *Listeria monocytogenes* is associated with increased resistance to  
355 surfactant sanitizers and heat. Journal of food protection 53, 550–554.
- 356 Fratamico, P.M., Annous, B.A., Guenther, N.W., 2009. Biofilms in the Food and Beverage Industries. Woodhead Publishing.
- 357 Freeman, C., Lock, M.A., Marxsen, J., Jones, S.E., 1990. Inhibitory effects of high molecular weight dissolved organic matter  
358 upon metabolic processes in biofilms from contrasting rivers and streams. Freshwater Biology 24, 159–166.
- 359 Galiè, S., García-Gutiérrez, C., Miguélez, E.M., Villar, C.J., Lombó, F., 2018. Biofilms in the food industry: Health aspects  
360 and control methods. Frontiers in microbiology 9, 898.
- 361 Hilloulin, B., Zhang, Y., Abraham, O., Loukili, A., Grondin, F., Durand, O., Tournat, V., 2014. Small crack detection in  
362 cementitious materials using nonlinear coda wave modulation. NDT & E International 68, 98–104. doi:10.1016/j.ndteint.  
363 2014.08.010.
- 364 InVs, 2016. Surveillance des toxi-infections alimentaires collectives, in: Données de la déclaration obligatoire.
- 365 Lens, P., O'Flaherty, V., Moran, A.P., Stoodley, P., Mahony, T., 2003. Biofilms in Medicine, Industry and Environmental  
366 Biotechnology. IWA Publishing.
- 367 Lohr, K.R., Rose, J.L., 2003. Ultrasonic guided wave and acoustic impact methods for pipe fouling detection. Journal of Food  
368 Engineering 56, 315–324. doi:10.1016/S0260-8774(02)00156-5.
- 369 MARTY, P., 2001. Maîtrise de la consommation d'eau dans les industries agro-alimentaires: Dossier eau. Industries alimentaires  
370 et agricoles 118, 35–39.
- 371 Matsumoto, S., Obara, K., Yoshimoto, K., Saito, T., Ito, A., Hasegawa, A., 2001. Temporal change in P-wave scatterer  
372 distribution associated with the M6.1 earthquake near Iwate volcano, northeastern Japan. Geophysical Journal International

- 373 145, 48–58. doi:10.1111/j.1365-246X.2001.00339.x.
- 374 Merheb, B., Nassar, G., Nongaillard, B., Delaplace, G., Leuliet, J.C., 2007. Design and performance of a low-frequency non-  
375 intrusive acoustic technique for monitoring fouling in plate heat exchangers. *Journal of Food Engineering* 82, 518–527.  
376 doi:10.1016/j.jfoodeng.2007.03.022.
- 377 Mussalli, Y.G., Hecker, G., Padmarabhan, M., Kasper, J., Chow, W., 1985. Targeted chlorination, in: *Condenser Biofouling*  
378 *Control Symposium: The State of the Art. Lake Buena Vista Florida. EPRI Report, 27pp.*
- 379 Olsson, A.L., Mitzel, M.R., Tufenkji, N., 2015. QCM-D for non-destructive real-time assessment of *Pseudomonas aeruginosa*  
380 biofilm attachment to the substratum during biofilm growth. *Colloids and Surfaces B: Biointerfaces* 136, 928–934.
- 381 Payan, C., Garnier, V., Moysan, J., Johnson, P.A., 2009. Determination of third order elastic constants in a complex solid  
382 applying coda wave interferometry. *Applied Physics Letters* 94, 011904. doi:10.1063/1.3064129.
- 383 Planès, T., Larose, E., 2013. A review of ultrasonic Coda Wave Interferometry in concrete. *Cement and Concrete Research* 53,  
384 248–255. doi:10.1016/j.cemconres.2013.07.009.
- 385 Ratdompurbo, A., Poupinet, G., 1995. Monitoring a temporal change of seismic velocity in a volcano: Application to the 1992  
386 eruption of Mt. Merapi (Indonesia). *Geophysical Research Letters* 22, 775–778. doi:10.1029/95GL00302.
- 387 da Silva, J.J., Wanzeller, M.G., Farias, P.d.A., Neto, J.S.d.R., 2008. Development of Circuits for Excitation and Reception in  
388 Ultrasonic Transducers for Generation of Guided Waves in Hollow Cylinders for Fouling Detection. *IEEE Transactions on*  
389 *Instrumentation and Measurement* 57, 1149–1153. doi:10.1109/TIM.2007.915480.
- 390 Snieder, R., 2002. Coda wave interferometry and the equilibration of energy in elastic media. *Physical Review E* 66, 046615.  
391 doi:10.1103/PhysRevE.66.046615.
- 392 Snieder, R., 2004. Extracting the Green's function from the correlation of coda waves: A derivation based on stationary phase.  
393 *Physical Review E* 69, 046610. doi:10.1103/PhysRevE.69.046610.
- 394 Sprung, C., Wählich, D., Hüttl, R., Seidel, J., Meyer, A., Wolf, G., 2009. Detection and monitoring of biofilm formation in  
395 water treatment systems by quartz crystal microbalance sensors. *Water Science and Technology* 59, 543–548.
- 396 Tandon, N., Choudhury, A., 1999. A review of vibration and acoustic measurement methods for the detection of defects in  
397 rolling element bearings. *Tribology International* 32, 469–480. doi:10.1016/S0301-679X(99)00077-8.
- 398 Van Asselt, A.J., Vissers, M.M.M., Smit, F., De Jong, P., 2005. In-line control of fouling, in: *Proceedings of Heat Exchanger*  
399 *Fouling and Cleaning-Challenges and Opportunities, Engineering Conferences International, Kloster Irsee, Germany.*
- 400 Van Houdt, R., Michiels, C., 2010. Biofilm formation and the food industry, a focus on the bacterial outer surface. *Journal of*  
401 *Applied Microbiology* 109, 1117–1131. doi:10.1111/j.1365-2672.2010.04756.x.
- 402 Withers, P., 1994. Ultrasonic sensor for the detection of fouling in UHT processing plants. *Food Control* 5, 67–72. doi:10.  
403 1016/0956-7135(94)90088-4.
- 404 Withers, P.M., 1996. Ultrasonic, acoustic and optical techniques for the non-invasive detection of fouling in food processing  
405 equipment. *Trends in Food Science & Technology* 7, 293–298. doi:10.1016/0924-2244(96)10031-5.
- 406 Zhang, Y., 2013. *Contrôle de Santé Des Matériaux et Structures Par Analyse de La Coda Ultrasonore*. Ph.D. thesis. Université  
407 du Maine.
- 408 Zhou, R., Huang, L., Rutledge, J.T., Fehler, M., Daley, T.M., Majer, E.L., 2010. Coda-wave interferometry analysis of time-  
409 lapse VSP data for monitoring geological carbon sequestration. *International Journal of Greenhouse Gas Control* 4, 679–686.  
410 doi:10.1016/j.ijggc.2010.01.010.